Les Cahiers du GERAD ISSN: 0711–2440

Balancing supply and demand in the presence of renewable generation via demand response for electric water heaters

A. I. Tammam, M. F. Anjos, M. Gendreau

G–2017–32

May 2017

GERAD HEC Montréal
3000, chemin de la Côte-Sainte-Catherine
Montréal (Québec) Canada H3T 2A7

Tél. : 514 340-6053
Téléc. : 514 340-5665
info@gerad.ca
www.gerad.ca

Balancing supply and demand in the presence of renewable generation via demand response for electric water heaters

Adham I. Tammam [a]
Miguel F. Anjos [a]
Michel Gendreau [b]

[a] *GERAD & Department of Mathematics and Industrial Engineering, Polytechnique Montréal (Québec) Canada, H3C 3A7*

[b] *CIRRELT & Department of Mathematics and Industrial Engineering, Polytechnique Montréal (Québec) Canada, H3C 3A7*

miguel-f.anjos@polymtl.ca
michel.gendreau@polymtl.ca

May 2017

Les Cahiers du GERAD
G–2017–32

Abstract: With the increasing penetration of renewable energy sources in the electrical power grid, demand response via thermostatic appliances such as electric water heaters is a promising storage means to compensate the significant variability in renewable generation power. We propose a multi-stage stochastic optimization model that computes the optimal day-ahead target profile of the mean thermal energy contained in a large population of heaters, given various possible wind power production and uncontrollable load scenarios, where this optimal profile is calculated to make the variable net demand as flat as possible.

Keywords: Direct load control, stochastic optimization, demand response, electric water heaters

Acknowledgments: This work was funded by an ECO Energy Innovation Initiative grant from Natural Resources Canada, and by the NSERC Energy Storage Technologies (NEST) Strategic Network.

1 Introduction

Although renewable energy sources are considered an expensive source of energy in terms of equipments, installation and maintenance compared to thermal resources, their increasing use in electrical grids is mainly due to the desire to reduce greenhouse gases emissions from burning fossil fuels for electricity, heat, and transportation. Yet the intermittency of renewables creates challenges for system operators who must ensure the balance at all times between supply (constrained by its ramping limits) and demand.

Demand-side management of energy storage in the form of thermostatically controlled appliances (TCAs), such as water heaters, space heaters, or batteries of electric vehicles, whose load curve can be reshaped while respecting the end-user comfort constraints, is a promising means to counterbalance the intermittence of renewables and has been the focus of many studies. Dynamic programming models have been developed to minimize the peak load considering deterministic load demand [1, 2, 3]. A control algorithm for TCAs to follow regulation signals in order to stabilize a network supplied with renewable resources was proposed in [4]. TCAs load shifting from peak to off-peak periods based on fuzzy logic control strategy can be found in [5, 6].

In this paper, we focus on studying the potential for controlling the electric water heaters load because of their ability to store energy for a considerable amount of time due to their high thermal inertia. Their peak of demand coincides with the peak of total load demand, which means that a significant reduction of the peak of the load curve could be achieved [7]. Finally, according to Natural Resources Canada, the power consumption of water heaters in Canada is important and could go up to 21.7% of the total demand load [8].

A deterministic linear optimization model which decides the number of water heaters to which one control scheme from a predefined set of schemes should be applied in order to reduce the peak load is proposed in [9]. A column generation approach is applied to a load management problem where the objective is to minimize the maximum peak of a known load profile by choosing among a large set of admissible interruption scenarios established in advance [10]. A metaheuristic algorithm based on particle swarm optimization to operate the power consumption of water heaters in order to shave the load curve is proposed in [7, 11]. Directly controlling the power consumption of residential water heaters could be used to reduce the power losses in an electric grid as in [12].

The aforementioned studies deal with the problem parameters in a deterministic setting, yet in reality load demand and renewable supply are uncertain. In [13], a centralized direct load control of electric water heaters (EWHs) was proposed in order to reduce the peak imports and exports on the Czech electricity market. The presented approach takes into account the stochastic nature of load demand and renewable production, hence the dispatch of the EWHs is decided through a two-stage stochastic optimization program, where the first stage computes the overall EWH load, and the second stage rectifies the dispatch according to the actual power supply and demand.

Multiple challenges arise when trying to control a huge number of storage devices individually small in capacity but diversified in their state, and spread throughout a pervasive communication platform, because a control schedule applied indiscriminately can spoil their natural load diversity, inducing the payback phenomenon that may create new peak loads [10]. Moreover centrally controlling a large population of storage devices discriminately requires sophisticated mathematical models and significant computational power to solve them.

For those aforementioned reasons, we consider a demand response approach as a hierarchical control architecture in two phases. In the first phase, we optimally schedule the day-ahead load of a homogeneous aggregate model of the EWHs population, in the presence of two stochastic parameters: (1) the uncontrollable load (the total load after excluding the controllable demand of EWHs) and (2) the renewable supply. We compute an optimal power profile (OPP) for this aggregate model, which is then translated into a temperature profile that specifies a series of hourly setpoints that the hot water is required to reach, in order to flatten the variable net load. In the second phase, a local control module sends instructions to individual EWHs so as to ensure that the mean thermal energy of the EWHs population follows the target from the OPP. This local controller proposed in [14] is based on the mean field theory and will be denoted by mean field controller

(MFC). This second phase is out of the scope of this paper, and the reader is refereed to [14, 15] for more information.

We propose a multistage stochastic optimization model, denoted by *Scheduler* through the rest of the paper, that computes the OPP on a rolling horizon basis. At the beginning, the scheduler receives the actual energy capacity of the EWHs, information regarding the actual total demand as well as the wind production. It then computes the optimal OPP that minimizes the mean variation of the net demand over the scenario tree over T time periods, only the optimal solution at the root node is sent to the MFC while omitting the rest of OPP. At the next time step, a new scenario tree is built with the same horizon's size, the scheduler receives an update of the actual EWHs energy capacity, actual total demand and wind production of the previous time step, and computes a new OPP over the new scenario tree, and only the solution at the root node is applied, and the system proceeds that way until the end of the horizon is reached.

The rest of this paper is organized as follows. In Section 2 we introduce the aggregate model of EWHs that will be used throughout the paper and illustrate the way to maintain feasibility of the OPP for the MFC. In Section 3 we present the *Scheduler*. In Section 5 we present a case study and the computational results. Section 6 concludes the paper.

2 Aggregate model of EWHs

Our optimization formulation is designed to work in conjunction with the mean field model proposed in [14], where each individual EWH is modeled by assuming that the reservoir is made up of n fully mixed equal volume layers, the cold water inlet is on the bottom layer and hot water is drawn from the top layer. Because the *Scheduler*'s formulation uses an aggregate model of EWHs by considering a group of homogeneous individual EWHs as one large thermal battery, modeling the EHWs as a single-layer large reservoir with a controllable mean water temperature given a sufficiently good approximation of the amount of energy that the EHW population is capable of absorbing as well as of the losses (mostly due to hot water draw events). Thermal energy conservation for the aggregate model of EWHs, also called the system dynamics, is expressed as:

$$e_{t+1} = e_t + x(e_t) - \ell(e_t) \tag{1}$$

where e_t is the stored energy (i.e., the system state) at time step t, $x(e_t)$ is the decision variable that represents the amount of energy one decides to inject into the reservoir, and which depends on the current system state, and $\ell(e_t)$ is the system loss due to heat transfer by conduction and the hot water extraction process.

The first component of the system loss term (i.e., heat transfer by conduction), denoted by $\ell_1(e_t)$, is defined as:

$$\ell_1(e_t) = KA\left(\frac{e_t}{C_p \rho V} + N_{ewh}(T_L - T_{env})\right) dt \tag{2}$$

where K is the thermal conductivity per unit length of EWHs, A is the summation of the surface areas of individual EWHs, C_p is the hot water specific heat, ρ is the water density, V is the summation of the volume of hot water in the EWHs, N_{ewh} is the number of individual EWHs represented in the aggregate model, T_L is the inlet water temperature, and T_{env} is the environment temperature.

Concerning the hot water extraction for an individual EWH, we adopted the model in [14] where water extraction is modeled as a continuous time Markov chain denoted by θ_t, $t \geq 0$, taking values in $\Theta = \{1, 2, \ldots, \mathfrak{I}\}$, with the identical infinitesimal generator $\Lambda = \{\lambda_{ij}, i, j, = 1, \ldots, \mathfrak{I}\}$, where each state consists of different drawn water volumes depending on the type of event such as shower, hand washing, etc. Knowing the probability of occurrence of each state, denoted by $\mathfrak{p}_i$ and defined as:

$$\begin{aligned} \mathfrak{p}_i &= \frac{\Pi_i}{\sum_{k=0}^{K} \Pi_k} \\ \Pi_0 = 1, \quad \Pi_i &= \frac{\lambda_{0,1}\lambda_{1,2}\ldots\lambda_{i-1,i}}{\lambda_{1,0}\lambda_{2,1}\ldots\lambda_{i,i-1}} \text{ for } i \geq 1, \end{aligned} \tag{3}$$

we can aggregate the losses due to hot water extraction by considering the expected flow of drawn hot water for each type of event i as follows:

$$\ell_2 = \rho C_p (T_{mix} - T_L) \sum_{i=1}^{\mathfrak{I}} N_{ewh} \mathfrak{p}_i \dot{V}_i^{mix} \tag{4}$$

where we suppose that the end-user mixes hot and cold water together to have the desired flow, denoted by $\dot{V}_i^{mix}$, and temperature, denoted by T_{mix}, depending on the type of extraction i.

The temperature within the reservoirs must be bounded below to prevent bacterial contamination (especially Legionella pneumophila whose growth potential is almost zero above 46°C [16]), and bounded above for end-user safety. The zone between those two bounds is the comfort zone, represented by the constraints (5):

$$\begin{aligned} e_{max} &= N_{ewh} \rho V C_p (T_{max} - T_L) \qquad \forall t, s \\ e_{min} &= N_{ewh} \rho V C_p (T_{min} - T_L) \qquad \forall t, s \end{aligned} \tag{5}$$

Therefore, the maximum amount of energy the system is able to absorb, $x(e_t)$, depends on its mean current state, e_t, because the nearer its mean current state is to the upper bound, the less energy it is able to accept, and vice versa. Moreover the EWHs will consume a minimum amount of energy to prevent the system from going below the lower limit of the comfort zone.

To bound the aggregate power consumption of EWHs, we considered the MFC module developed in [14] as a black box and used it to calculate the maximum and minimum electric power that the EWH population can consume for all reachable values of e_t. It is important to note that, for a certain energy level, not all members of the EWH population under control reach this exact same energy level, but they are rather distributed around it with a certain variance and skewness, where this distribution cannot be considered as a normal distribution due to the comfort zone constraint which trims the tails of the probability density function; furthermore the variance and skewness depend on the control. A study of the distribution of the EWH population state around a finite set of system state e_t was conducted so that we can randomly generate initial states of EWHs following this pre-calculated probability density function.

For every possible discrete value of a target energy level e_t, we begin the simulation assuming that the EWH population follows a normal distribution with mean μ and variance 1, the MFC is then asked to control the EWH population to make its mean energy state reach e_t. Once the population's mean converges to e_t, we calculate its variance and skewness around e_t, we denote this density function by f_{e_t}. Second, for every e_t, the state of EWH population is initialized so that its state distribution follows f_{e_t}. The MFC is then asked to get the mean population's temperature up to its lower and upper limits, T_{min} and T_{max} respectively, from which the lower and upper aggregate power consumption bounds are calculated.

Figures 1–3 show the distribution of the thermal energy of the population when its mean moves towards the lower bound, middle and upper bound of the comfort zone respectively. One can notice two things: (1) the thermal energy distribution has a clear negative skewness due to the hot water draw events that result in thermal losses and in a large portion of the EWHs to reach a temperature below the population's mean temperature, and (2) the distribution's variance shrinks whenever the mean gets closer to the bounds, which affects the population's diversity.

Figure 4 shows the simulated results of the maximum and minimum power consumption for 200 EWHs. The feasible region of $x(e_t)$ is the region between the two monotonically non-increasing functions. A linear regression is applied to the upper bound, as shown in Figure 5. For the lower bound, we use a convex quadratic regression, as shown in Figure 6; the resulting quadratic function is then outer approximated by a piecewise linear function formed using supporting hyperplanes.

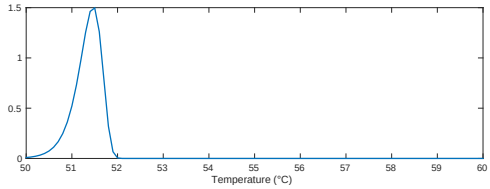

Figure 1: Population distribution near the lower bound

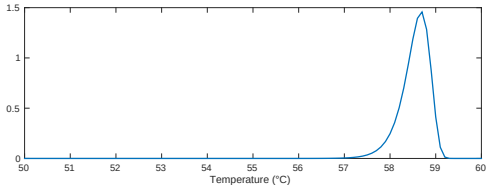

Figure 2: Population distribution near the upper bound

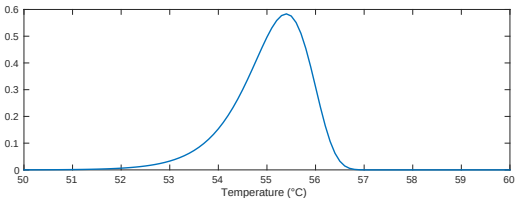

Figure 3: Population distribution at the middle of the comfort zone

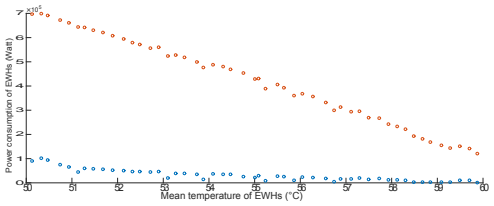

Figure 4: Simulated bounds

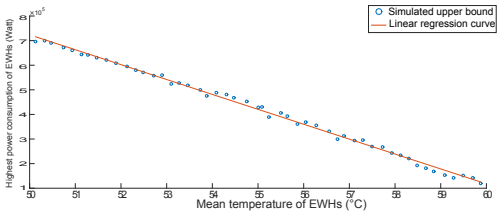

Figure 5: Linear regression for the upper bound

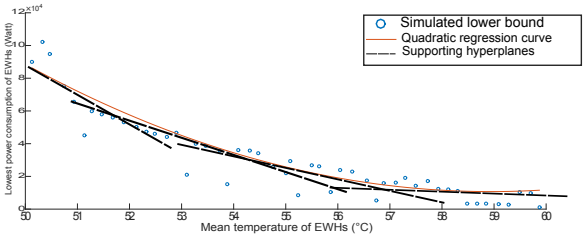

Figure 6: Quadratic regression for the lower bound

3 Stochastic model

Several optimization techniques have been developed to deal with problems that contain uncertain parameters, namely stochastic dynamic programming [17], robust optimization [18, 19, 20, 21], chance-constrained optimization [22], and stochastic optimization with recourse [23]. A review of different optimization approaches that solve problems having uncertain parameters can be found in [24].

Uncertain parameters are usually modeled either by distributions or by stochastic processes. The former is used when the decision is to be made over one stage, and the latter when a series of decisions have to be taken over multiple stages [25]. In our case, a series of decisions are to be taken for all hourly time steps in the planning horizon, and the two stochastic processes that we are dealing with are the uncontrollable demand and wind power production.

Stochastic optimization with recourse is our chosen approach. Except for certain special cases where the model is solvable directly with continuous distributions, most solution methods require discrete distributions of finite cardinality. The continuous random process therefore has to be approximated by a discrete finite set of outcomes in a form of *scenario tree* that represents the diffusion of stochastic information into the future. The tree represents the multiple stages of observation of the possible outcomes of the random variables in

time, and decisions are taken at different stages depending on the available data up the given stage, and regardless of future observations that are considered uncertain. As more observations are revealed, recourse decisions are made in order to rectify sub-optimal solutions that may result from decisions of previous stages.

Figure 7 illustrates an example of a scenario tree with three stages, where the root node is the value of the discrete stochastic process $\{\xi_t\}$ at $t = 0$ and considered deterministic (i.e., has a probability of occurrence equals to 1). Two possible outcomes at the next stage $t = 1$ are represented by two nodes with values ω_1 and ω_2, each of which can lead to two other possible realizations of the random process, (ω_3, ω_4) and (ω_5, ω_6) respectively, with their conditional probabilities shown on the arcs of the tree. Note that the number of stages in a scenario tree does not necessarily reflect the number of time steps in the optimization problem but rather the number of times that new observations of the random process are observed. The larger the size of the scenario tree, the better the representation of the uncertain stochastic process, but also the larger the optimization problem.

3.1 Mathematical model

The objective of the *Scheduler* is to flatten the net demand curve, denoted by p_n (in MW) and equal to the remaining demand after absorbing the renewable production that is dispatched with the highest priority. The means at our disposal is to compute the optimal electric power consumption of the controllable load of EWHs, denoted by $x_n(e_n)$ (in MWh), so that valleys are filled and peaks are shaved while respecting the end-user comfort. Net demand is expressed as

$$p_n = d(\omega_n) - r(\omega_n) + \frac{x_{\widehat{n}}(e_{\widehat{n}})}{\Delta t} \tag{6}$$

where $d(\omega_n)$, $r(\omega_n)$ are respectively observed values of the uncontrollable demand and the wind power production at node $n \in 1, \cdots, N$ of the scenario tree with N nodes(both in MW), and Δt is the discrete time step size. To respect the nonanticipativity conditions, the decision $x_{\widehat{n}}(e_{\widehat{n}})$ is taken at the parent node of node n in the scenario tree, denoted by $\widehat{n}$, before observing the realization of $d(\omega_n)$ and $r(\omega_n)$. At the root node d and r are deterministic (observed) parameters, where d is the actual total demand, and r is the actual wind power.

Flattening the net demand curve consists of minimizing the absolute value of the difference of the net demands at two consecutive nodes in the scenario tree multiplied by their probability of occurrence:

$$\min_{z \in \mathbb{R}^n} \quad \sum_{n=0}^{N} Pr_n z_n \tag{7}$$

where Pr_n is the absolute probability of occurrence of node n, and z_n is the absolute value of the difference between the net demands at node n and at its parent node $\widehat{n}$. We can model this absolute value using the following linear formulation:

$$z_n \geq p_n - p_{\widehat{n}}, \quad z_n \geq p_{\widehat{n}} - p_n. \tag{8}$$

The resulting stochastic optimization model is:

$$\begin{aligned}
\min_{z \in \mathbb{R}^n} \quad & \sum_{n=0}^{N} Pr_n z_n \\
\text{s.t.} \quad & z_n \geq p_n - p_{\widehat{n}} \quad \forall n \\
& z_n \geq p_{\widehat{n}} - p_n \quad \forall n \\
& p_n = d(\omega_n) - r(\omega_n) + \frac{x_{\widehat{n}}(e_{\widehat{n}})}{\Delta t} \quad \forall n \\
& e_n = e_{\widehat{n}} + x_{\widehat{n}}(e_{\widehat{n}}) - \ell(e_{\widehat{n}}) \quad \forall n \\
& \ell_1(e_n) = KA\left(\frac{e_n}{C_p \rho V} + N_{ewh}(T_L - T_{env})\right)\Delta t \quad \forall n
\end{aligned}$$

$$
\begin{aligned}
\ell_2 &= \rho C_p (T_{mix} - T_L) \sum_{i=1}^{\mathfrak{I}} N_{ewh} \mathfrak{p}_i \dot{V}_i^{mix} \\
\ell(e_{\widehat{n}}) &= \ell_1(e_n) + \ell_2 \\
e_o &= N \rho V C_p (T_{init} - T_L) \\
e_n &\leq N_{ewh} \rho V C_p (T_{\max} - T_L) \quad \forall n \\
e_n &\geq N_{ewh} \rho V C_p (T_{\min} - T_L) \quad \forall n \\
x_n(e_n) &\leq A_1(e_n) + B_1 \quad \forall n \\
x_n(e_n) &\geq \underline{Q}(e^i) + \mathring{\underline{Q}}(e^i)(e_n - e^i) \quad \forall n, i \\
x_n(e_n) &\geq 0 \\
e_n &\geq 0
\end{aligned}
$$

where we also included the bounds over $x_n(e_n)$ from the regression approximation.

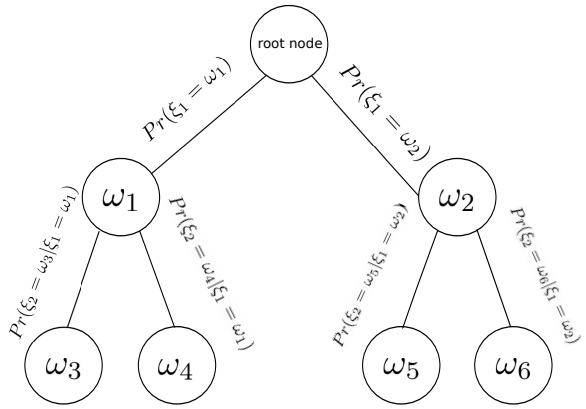

Figure 7: Three-stage scenario tree

4 Scenario generation

In this section we describe the steps to generate the multi-stage scenario tree for our stochastic optimization problem. Artelys, a company specialized in optimization, decision-support and modeling, cooperated with us by developing a load forecast model trained over a set of historical data of power consumption from 2012 to 2014 provided by supervisory control and data acquisition (SCADA) of the CoopÃl'rative RÃl'gionale d'ElectricitÃl' de Saint-Jean-Baptiste de Rouville (CoopSJB). The CoopSJB data are collected from five distribution substations in Mont Saint-Hilaire, a suburb of Montreal, for 6,819 houses. These data are normalized to get the mean power consumption per house. The forecast model takes as inputs the hourly wind speed and temperature of day d_k and the hourly forecast for day d_{k+1}, and outputs the hourly load demand forecast for d_{k+1}. Multiple load demand curves are generated using wind speed and temperature ensemble forecasts provided from Environment Canada that releases each day a set of 22 forecasts for the next 144 hours. The uncontrollable demand component is obtained by computing an estimate of the hourly consumption of EWHs using the data from CoopSJB, and subtracting this estimate from the total demand. Wind power scenarios are generated from the wind speed ensemble forecasts using the approach proposed in [26]. Every uncontrollable load demand scenario is coupled with its correspondent wind power scenario resulting from the same wind speed forecast.

In this way, a fan of scenarios is constructed with 22 scenarios and 24 nodes per scenario for the 24-hour horizon, where each node has two (hourly) values: uncontrollable demand and wind power production. A fan of scenarios does not reflect well the future uncertainty as it omits its nonanticipative property. For this reason we apply the forward construction algorithm described in [27] to the fan of scenarios to obtain a nonanticipative scenario tree.

5 Case study and results

The results presented here come from a case study developed in the context of the project **smartDESC** smart Distributed Energy Storage Controller), whose objective is to perform a proof of concept of a hierarchical control architecture to manage the power consumption of dispersed energy storage devices throughout the electric grid (such as electric water heaters, space heaters, or electric vehicles), in order to mitigate the intermittency in power production caused mainly by the increasing penetration of renewable energy resources. The reader is referred to [28] for further information about the project architecture.

5.1 Results

The aggregate model used throughout this case study represents a population of 200 EHWs; however the depicted curves in this section is averaged over 200 houses. The planning horizon is 24 hours long with hourly time steps. The rolling horizon approach was applied: at every time step t, a new scenario tree, denoted by $\{\xi_t\}_{t\in T}$, is created depending on the available wind speed and demand forecasts. Only the optimal solution $x^*_{0,t}$ at the root node $\xi_{0,t}$ of the scenario tree is considered and the solution for the rest of the scenario tree is omitted, where the root node contains the values of total demand and wind production actually observed from the previous time step $t-1$.

The wind power production scenarios are scaled so that the average of their maximum values over the planning horizon is equal to 10% of the average value of the maximum uncontrollable demand over the same horizon. This was done in order to test the load curve shaving the system can reach when the maximum wind power production is on average equal to 10% of the uncontrollable demand.

As previously mentioned, the root node of the scenario tree $\{\xi_t\}_{t\in T}$ contains the actual realization of the total demand and wind power, thus a deterministic observation of those two parameters has to be constructed over the planning horizon. We present three cases in which the mean uncontrollable demand forecast is considered as the observed uncontrollable demand, and this demand is coupled with three different wind power observations: maximum, average and minimum wind power. This is depicted in Figures 8–10, where the upper curve is the uncontrolled demand, the lower curve is the net demand, and the region in cyan between them represents the magnitude of wind power.

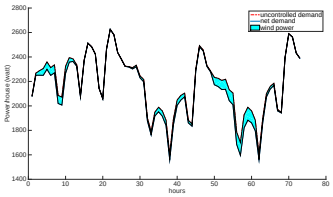

Figure 8: Case study with minimum wind power

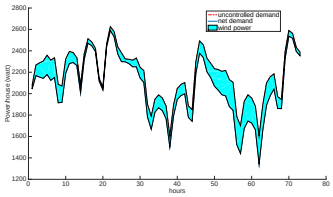

Figure 9: Case study with average wind power

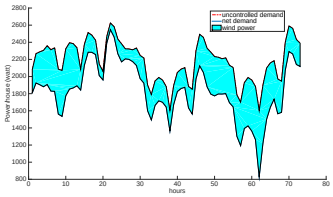

Figure 10: Case study with maximum wind power

Figures 11–13 depict the load shaving curves with low, average and high wind penetration, where the total target power curve is the EWH optimal power consumption that the *Scheduler* computes, whereas the total simulated power curve is the real EWH power consumption the MFC is able to achieve. These graphs show that in general the target power consumption profile generated by the *Scheduler* is feasible with respect to the MFC (i.e., the EWH simulated power curve and the EWH target power curve are almost overlapped); however in some parts of the graph, the MFC power consumption deviates from the target power profile. A solution for this problem was developed and will be reported in our next paper.

Table 1 shows the peak reduction resulting from the direct control of the power consumption of the EWH population as a percentage of the peak of load in the thermostatic control mode (third column); the reduction in demand variance as a percentage of the demand with the thermostatic control of EWHs (forth column); and the computational time required to solve the stochastic optimization problem with rolling horizon (last

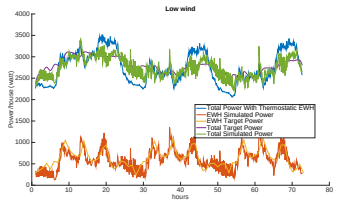

Figure 11: Load shaving with low wind power

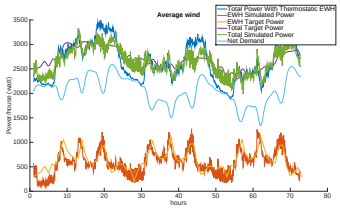

Figure 12: Load shaving with average wind powe

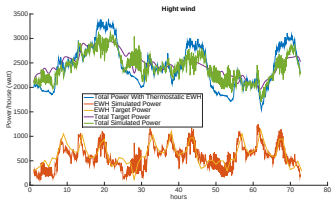

Figure 13: Load shaving with high wind power

column). The reduction in demand variance is an estimate of how well the net demand curve is flattened. It is obvious that as wind power is added to the grid, the greater the variation in the net demand, and the more challenging it is to manage the EWH load to reduce the demand fluctuation. This is illustrated by comparing the net demand variation reduction for every wind blow scenario when the mean wind penetration is 10% versus 20% in Table 1.

Table 1: Comparison between 3 cases of wind blow for 10% and 20% of wind power penetration during 3 days

Wind Penetration	Wind blow	Peak Shaving (%)	Net Demand Variation Reduction (%)	Time (sec)
10%	High Wind	6.68	46.40	21.535
	Average Wind	7.85	49.42	21.471
	Low Wind	7.84	50.82	21.454
20%	High Wind	6.51	32.82	22.674
	Average Wind	8.57	42.60	21.849
	Low Wind	8.46	45.16	22.544

Two other observations are important to make. First, Figure 14 shows that when the wind power penetration to the grid increases, the net demand load curve fluctuation reduction decreases; this is because of the limited storage capacity of EWHs to absorb the wind power intermittence. On the other hand, Figure 15 illustrates how this increase in wind power permits the operator to reduce its peak of the load curve, though eventually this gain in peak reduction decreases as the penetration of renewables increases. These results were obtained with a participation of 100% of the population of EWHs in the demand response program.

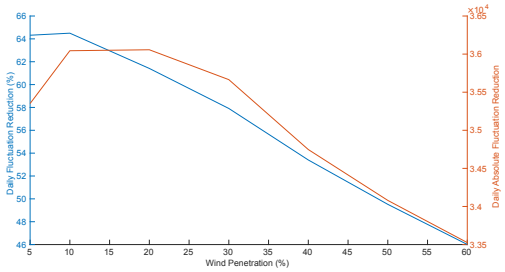

Figure 14: Reduction of Daily Fluctuation versus Wind Penetration

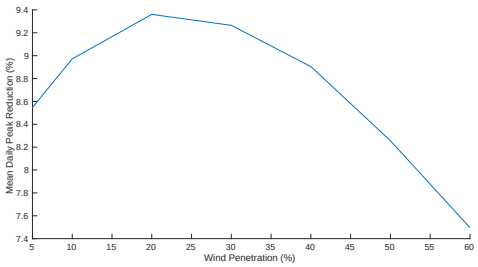

Figure 15: Mean Daily Peak Reduction versus Wind Penetration

6 Conclusion

In this article we proposed a multi-stage stochastic optimization model for load shaving in the presence of renewable resources attached to the grid, by mean of the storage capacity of residential electric water heaters. This model is a part of the project smartDESC that offers a hierarchical control architecture that controls dispersed controlled devices locally and more efficiently while achieving the global system operator goals of peak shaving and net demand flattening. The model shows the impact of renewable upon the variability of net demand curve which gives the system operator an idea about how much renewable power it can afford while maintaining a stable and servable demand.

References

[1] R. Bischke and R. A. Sella, "Design and controlled use of water heater load management," Power Apparatus and Systems, IEEE Transactions on, PAS-104(6) 1290–1293, 1985.

[2] A. I. Cohen and C. Wang, "An optimization method for load management scheduling," Power Systems, IEEE Transactions on, 3(2) 612–618, 1988.

[3] L. Zhang and Y. Li, "Optimal energy management of wind-battery hybrid power system with two-scale dynamic programming," Sustainable Energy, IEEE Transactions on, 4(3) 765–773, July 2013.

[4] J. Kondoh, N. Lu, and D. Hammerstrom, "An evaluation of the water heater load potential for providing regulation service," Power Systems, IEEE Transactions on, 26(3) 1309–1316, 2011.

[5] M. Nehrir and B. LaMeres, "A multiple-block fuzzy logic-based electric water heater demand-side management strategy for leveling distribution feeder demand profile," Electric Power Systems Research, 56(3) 225–230, 2000. [Online]. Available: http://www.sciencedirect.com/science/article/pii/S0378779600001243

[6] B. LaMeres, M. Nehrir, and V. Gerez, "Controlling the average residential electric water heater power demand using fuzzy logic," Electric Power Systems Research, 52(3) 267–271, 1999. [Online]. Available: http://www.sciencedirect.com/science/article/pii/S037877969900022X

[7] A. Sepulveda, L. Paull, W. Morsi, H. Li, C. Diduch, and L. Chang, "A novel demand side management program using water heaters and particle swarm optimization," in Electric Power and Energy Conference (EPEC), 2010 IEEE, 2010, 1–5.

[8] Energy Use Data Handbook. Natural Resources Canada, June 2004.

[9] S. H. Lee and C. L. Wilkins, "A practical approach to appliance load control analysis: A water heater case study," Power Apparatus and Systems, IEEE Transactions on, PAS-102(4) 1007–1013, 1983.

[10] J.-C. Laurent, G. Desaulniers, R. Malhame, and F. Soumis, "A column generation method for optimal load management via control of electric water heaters," Power Systems, IEEE Transactions on, 10(3) 1389–1400, 1995.

[11] P. A. Rosario, W. Morsi, and L. Chang, "Application of pso to optimize the operation of electric water heaters for reserve provision," in Electrical Power and Energy Conference (EPEC), 2011 IEEE, 2011, 164–169.

[12] H. Salehfar and A. Wehbe, "Direct control of residential water heater loads to reduce power system distribution losses," in Power Engineering Society Winter Meeting, 2001. IEEE, 3, 2001, 1455–1460 3.

[13] O. Malik and P. Havel, "Active demand-side management system to facilitate integration of renewable energy sources (RES) in low-voltage distribution networks," Sustainable Energy, IEEE Transactions on, 5(2) 673–681, April 2014.

[14] A. Kizilkale and R. Malhame, "Collective target tracking mean field control for markovian jump-driven models of electric water heating loads," Groupe d'Etudes et de Recherche en Analyse des Decisions (GERAD), Tech. Rep., 2014.

[15] A. C. Kizilkale and R. P. MalhamÃl', "Mean field based control of power system dispersed energy storage devices for peak load relief," in Decision and Control (CDC), 2013 IEEE 52nd Annual Conference on, Dec 2013, 4971–4976.

[16] M. Lacroix, "Electric water heater designs for load shifting and control of bacterial contamination," Energy Conversion & Management, 40, 1313–1340, 1999.

[17] D. P. Bertsekas, Dynamic Programming and Optimal Control. Athena Scientific; 4th edition, 2007.

[18] A. Ben-Tal and A. Nemirovski, "Robust solutions of linear programming problems contaminated with uncertain data," Mathematical Programming, 88(3) 411–424, 2000. [Online]. Available: http://dx.doi.org/10.1007/PL00011380

[19] D. Bertsimas, D. B. Brown, and C. Caramanis, "Theory and applications of robust optimization," SIAM Review, 53(3) 464–501, 2011. [Online]. Available: http://dx.doi.org/10.1137/080734510

[20] D. Bertsimas and M. Sim, "The price of robustness," Operations research, 52(1) 35–53, 2004.

[21] R. Ferreira, L. Barroso, and M. Carvalho, "Demand response models with correlated price data: A robust optimization approach," Applied Energy, 96(0) 133 – 149, 2012, smart Grids. [Online]. Available: http://www.sciencedirect.com/science/article/pii/S0306261912000220

[22] G. Dorini, P. Pinson, and H. Madsen, "Chance-constrained optimization of demand response to price signals," Smart Grid, IEEE Transactions on, 4(4) 2072–2080, Dec 2013.

[23] J. Birge and F. Louveaux, Introduction to Stochastic Programming, ser. Springer Series in Operations Research and Financial Engineering. Springer, 2011. [Online]. Available: http://books.google.ca/books?id=Vp0Bp8kjPxUC

[24] N. V. Sahinidis, "Optimization under uncertainty: state-of-the-art and opportunities," Computers & Chemical Engineering, 28(6–7) 971–983, 2004, {FOCAPO} 2003 Special issue. [Online]. Available: http://www.sciencedirect.com/science/article/pii/S0098135403002369

[25] M. Kaut and S. W. Wallace, "Evaluation of scenario-generation methods for stochastic programming," in World Wide Web, Stochastic Programming E-Print Series, 2003, 14–2003.

[26] A. I. Tamam, C. S. Watters, M. F. Anjos, and M. Gendreau, "A methodology for ensemble wind power scenarios generation from numerical weather predictions (accepted for ieee pes gm 2016 proceedings)," GERAD, Tech. Rep., 2015.

[27] H. Heitsch and W. Römisch, "Scenario tree modeling for multistage stochastic programs," Mathematical Programming, 118(2) 371–406, 2007. [Online]. Available: http://dx.doi.org/10.1007/s10107-007-0197-2

[28] K. A. C. et al., "smartdesc: Smart distributed energy storage controller (in preparation)."